Sol−Gel Synthesis of Thick Ta_2O_5 Films

Nicholas Ndiege,[†] Tabitha Wilhoite,[†] Vaidyanathan Subramanian,[†,§] Mark A. Shannon,[‡] and Richard I. Masel*[†]

Department of Chemical and Biomolecular Engineering and Department of Mechanical Science and Engineering, University of Illinois at Urbana−Champaign, 600 South Mathews Street, Urbana, Illinois 61801

Received September 18, 2006. Revised Manuscript Received March 6, 2007

Advances in microelectromechanical systems have generated an ever-growing demand for novel insulating material applicable to high-temperature systems. Ta_2O_5 is appealing for such applications because of its high index of refraction, refractory nature, and negligible absorbance in the infrared region. The challenge faced in the realization of such materials is the synthesis of crack-free Ta_2O_5 films whose thickness is on the order of a quarter wavelength of the incident infrared radiation. This work seeks to investigate the effect of addition of polyvinyl pyrollidone (PVP) as a binder material in the presence of 2-methoxyethanol and acetylacetone in the sol−gel synthesis of thick, uniform, and crack-free Ta_2O_5 films. Incorporation of PVP into the sol precursor has enabled uniform and crack-free films with thicknesses of up to 2.4 μm to be realized. Chemical probing of the precursor was conducted via TGA, FTIR, and NMR analysis of the sol to elucidate the processes behind this film formation, showing that the PVP hydrogen-bonds with the growing oxide but does not affect the sol chemistry. Instead, the PVP prevents crack formation, probably by relieving stresses in the film.

Introduction

Insulation for high-temperature microelectromechanical systems has become a key area in research because of the development of microreactor systems that can attain wall temperatures on the order of 1200 °C.[1,2] To add utility and portability to such systems, it is required that parts of composite devices that incorporate such high-temperature components be thermally isolated. Refractory blocks (e.g., fibrous alumina) on the centimeter order of thickness are the best mode of insulation currently available.

Photonic crystals have demonstrated a tunabilty such as to exhibit a photonic band gap in the infrared wavelength.[3] This is promising, because at temperatures above 600 °C, IR radiation is the dominant mode of heat loss.[4,5] Thus, multilayer quarterwave photonic structures can be explored to not only effectively insulate but also to anisotropically expel heat generated by microreactors.

The greatest challenge posed in realizing such materials is that photonic crystals with a band gap in the IR calls for structures made out of dense refractory material with thicknesses ranging from 1 to 5 μm.[3] Ta_2O_5 is the material of choice because of its high index of refraction, refractory nature, and negligible absorbance in the infrared region.[4,6,7] Current deposition techniques typically attain thicknesses on the order of 1−1.5 μm.[7−14] Furthermore, these are achieved by use of high cost systems such as chemical vapor deposition, e-beam deposition, etc. Any attempts at thicknesses beyond this range are hampered by very slow growth rates, film buckling, cracking, and even catastrophic delamination.[9,15,16] Sol−gel synthesis techniques are appealing because of their low cost and flexibility with regards to chemical tuning of the properties of the final material sought. Binder molecules such as ethylcellulose, polyethyleneimine (PEI), polyvinyl pyrollidone (PVP), and polyvinyl butyral (PVB) have been shown to increase film thickness with little or no cracking when incorporated in the sol precursor.[17−22]

* Corresponding author. E-mail: r-masel@uiuc.edu.
[†] Department of Chemical and Biomolecular Engineering, University of Illinois at Urbana−Champaign.
[‡] Department of Mechanical Science and Engineering, University of Illinois at Urbana−Champaign.
[§] Current address: at Chemical & Metallurgical Engineering, University of Nevada, Reno, NV.

(1) Ganley, J. C.; Seebauer, E. G.; Masel, R. I. *Aiche J.* **2004**, *50* (4), 829−834.
(2) Ganley, J. C.; Thomas, F. S.; Seebauer, E. G.; Masel, R. I. *Catal. Lett.* **2004**, *96* (3−4), 117−122.
(3) Fleming, J. G.; Lin, S. Y.; El-Kady, I.; Biswas, R.; Ho, K. M. *Nature* **2002**, *417* (6884), 52−55.
(4) Hass, D. D. P. D.; Glass, D. E.; Wiedemann, K. E. *Reflective Coating on Fibrous Insulation for Reduced Heat Transfer*; NASA Contractor Report 201733; National Aeronautics and Space Administration Langley Research Center: Hampton, VA, August 1997.
(5) Viskanta, R. *Int. J. Eng. Sci.* **1998**, *36* (12−14), 1677−1699.
(6) Mir, J. M.; Agostinelli, J. A. *J. Vac. Sci. Technol., A* **1994**, *12* (4), 1439−1445.
(7) Ozer, N.; Lampert, C. M. *J. Sol−Gel Sci. Technol.* **1997**, *8* (1−3), 703−709.
(8) Ezhilvalavan, S.; Tseng, T. Y. *J. Mater. Sci.: Mater. Electron.* **1999**, *10* (1), 9−31.
(9) Chaneliere, C.; Autran, J. L.; Devine, R. A. B.; Balland, B. *Mater. Sci. Eng., R* **1998**, *22* (6), 269−322.
(10) Beinhorn, F.; Ihlemann, J.; Simon, P.; Marowsky, G.; Maisenholder, B.; Edlinger, J.; Neuschafer, D.; Anselmetti, D. *Appl. Surf. Sci.* **1999**, *139*, 107−110.
(11) Kukli, K.; Aarik, J.; Aidla, A.; Kohan, O.; Uustare, T.; Sammelselg, V. *Thin Solid Films* **1995**, *260* (2), 135−142.
(12) Corbella, C. V. M.; Pinyol, A.; Porqueras, C.; Person, C.; Bertran, E. *Solid State Ionics* **2003**, *165*, 15−22.
(13) Toki, K.; Kusakabe, K.; Odani, T.; Kobuna, S.; Shimizu, Y. *Thin Solid Films* **1996**, *282* (1−2), 401−403.
(14) Werder, D. J.; Kola, R. R. *Thin Solid Films* **1998**, *323* (1−2), 6−9.
(15) Joshi, P. C.; Cole, M. W. *J. Appl. Phys.* **1999**, *86* (2), 871−880.
(16) Liu, L.; Wang, Y.; Gong, H. *J. Appl. Phys.* **2001**, *90* (1), 416−420.

10.1021/cm062231w CCC: $37.00
Published on Web 05/26/2007

In a previous study, we showed that incorporation of PVP and acetylacetone in a Ta_2O_5 sol allows one to produce dense, 2.4 μm thick Ta_2O_5 films on silicon with negligible cracking. Also observed are changes in film microstructure as the sol ages.[23] These films retained their stability even after prolonged heating at high temperature. Despite these discoveries, the mechanisms by which the constituent molecules facilitate the superior quality of oxide films still remain to be understood. Hence, in this paper, we seek to investigate the interactions between PVP, 2-methoxyethanol, and acetylacetone that make up the tantalum complex used in the preparation of thick Ta_2O_5 films. The sol precursors were analyzed with time from the point of synthesis until 20 days later. Chemical probing was performed via FTIR and NMR analysis. Thermogravimetric analysis (TGA) of the sol precursor was also performed. The resulting oxide films were characterized via scanning electron microscopy (SEM), X-ray diffraction (XRD), and X-ray photoelectron spectroscopy (XPS). The binder was found to have a viscosity-increasing effect when incorporated into the sol precursor. This allowed for thicker films due to the increased surface tension during spin or dip coating. PVP also reduces the rate of solvent expulsion from the wet film via hydrogen-bond formation. It also hydrogen-bonds with the growing metal−oxide network, both of which limit crack formation during drying and calcination.[18,24]

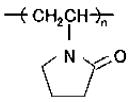

Experimental Section

Sol Synthesis. Figure 1 shows a schematic of the sol synthesis. 1-Propanol (99+%) was added to tantalum(V) ethoxide (99.98%) in a 100 mL round-bottomed flask with stirring to prevent rapid hydrolysis of the latter when exposed to ambient moisture. PVP (avg MW = 1,300,000) was weighed out in a beaker to which 2-methoxyethanol (99.3+%) was added with stirring (molecular weight of PVP monomer was used in the calculations). The mixture was further sonicated for 15 min to achieve complete binder dissolution. The PVP/2-methoxyethanol solution was then added to the tantalum(V) ethoxide/1-propanol solution with stirring. The resulting mixture was refluxed for 2 h at 130 °C. This was followed by vacuum evaporation until a 12% loss in mass was attained. The solution was cooled to room temperature, after which acetylacetone (99+%) was added, yielding a yellow colored solution. The solution was stirred for 20 h in a capped flask. This resulting sol was used for deposition by spin coating at various age points. Further details

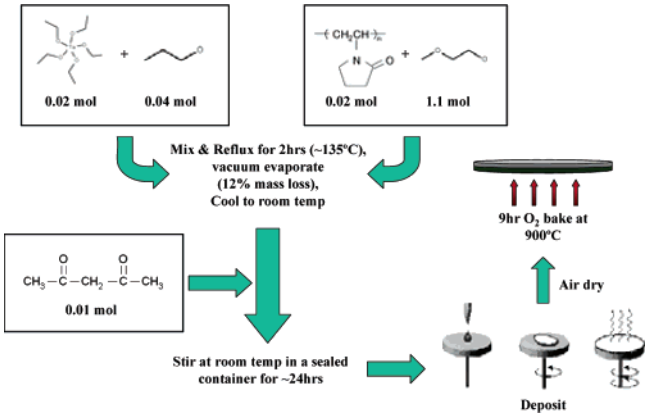

Figure 1. Sol−gel scheme of synthesis and deposition of Ta_2O_5. See text.

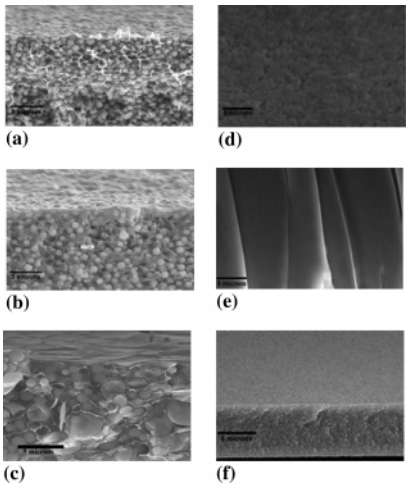

Figure 2. SEM micrographs of green Ta_2O_5 films on Si <111> deposited from sols of varying age: (a−c) sol with acetylacetone; (d−f) sol without acetylacetone (scale bars = 5 μm).

are discussed elsewhere.[23] The films were then left to dry in air for 24 h and subjected to a 9 h bake at 900 °C under an O_2 flow of 100 cm^3/min. The temperature ramping rate was 1.6 °C/min for both up and down cycles.

Control samples were synthesized as above but with modifications as follows:

- Without PVP ($Ta(OC_2H_5)_5$, isopropanol, acetylacetone, 2-methoxyethanol)
- Without acetylacetone ($Ta(OC_2H_5)_5$, isopropanol, PVP, 2-methoxyethanol)

Results

SEM Analysis. Figure 2 shows representative scanning electron picroscopy (SEM) pictures of samples of green (uncalcined) films to examine the microstructure resulting from the sols of different ages. Analysis was performed on JEOL 6060LV and HITACHI S4700 SEM machines. Generally, in the absence of acetylacetone, one observes crack-free films with no apparent structure. When the film is cleaved, the cleavage plane looks rough and shear lines are sometimes seen, but no clear structure is apparent. In contrast, when acetylacetone is added, the morphology changes. There are small rounded nodules containing tantalum held in a porous matrix. The nodules grow as the film ages. At the end of 20 days, the nodules are 2−5 μm across in diameter.

FTIR Analysis. Figure 3 shows an FTIR spectrum of a sol containing acetylacetone. A comparison spectrum of the

(17) Kozuka, H.; Takenaka, S.; Tokita, H.; Okubayashi, M. *J. Eur. Ceram. Soc.* **2004**, *24* (6), 1585−1588.
(18) Kozuka, H.; Kajimura, M.; Hirano, T.; Katayama, K. *J. Sol−Gel Sci. Technol.* **2000**, *19* (1−3), 205−209.
(19) Chen, W.; Zhang, J. Y.; Fang, Q.; Li, S.; Wu, J. X.; Li, F. Q.; Jiang, K. *Sens. Actuators, B* **2004**, *100* (1−2), 195−199.
(20) Chen, Y. Y.; Wei, W. C. J. *J. Eur. Ceram. Soc.* **2001**, *21* (14), 2535−2540.
(21) Jia, Q. X.; Mccleskey, T. M.; Burrell, A. K.; Lin, Y.; Collis, G. E.; Wang, H.; Li, A. D. Q.; Foltyn, S. R. *Nat. Mater.* **2004**, *3* (8), 529−532.
(22) Kishimoto, T.; Kozuka, H. *J. Mater. Res.* **2003**, *18* (2), 466−474.
(23) Subramanian, V.; Ndiege, N.; Seebauer, E. G.; Shannon, M. A.; Masel, R. I. *Thin Solid Films* **2007**, in press.
(24) Fidalgo, A.; Ilharco, L. M. *J. Sol−Gel Sci. Technol.* **2003**, *26* (1−3), 363−367.

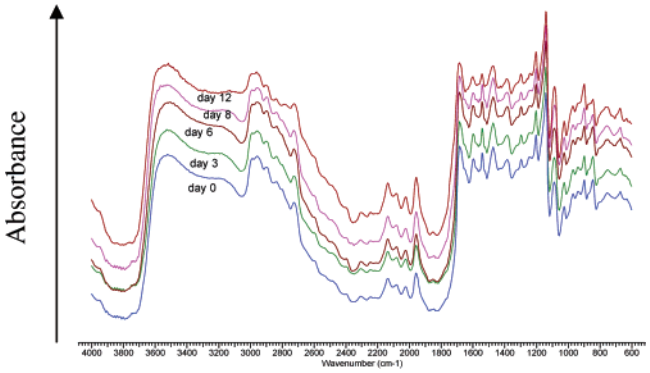

Figure 3. FTIR spectra of dip-coated film made from a sol containing acetylacetone.

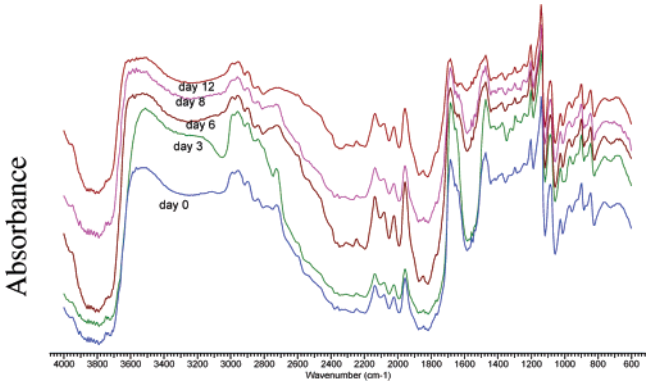

Figure 4. FTIR spectra of a dip-coated film made from sol with no acetylacetone.

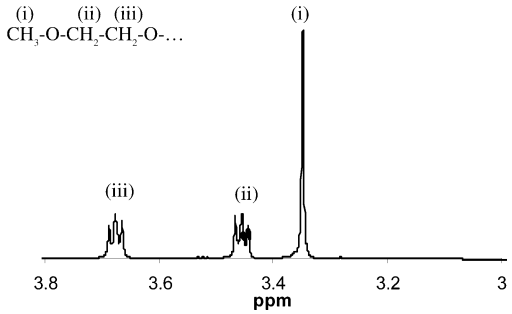

Figure 5. ^{1}H NMR of a sol made from $Ta(OC_2H_5)_5$, isopropanol, PVP, acetylacetone, and 2-methoxyethanol before deposition.

sols without acetylacetone is shown in Figure 4. Sampling for FTIR was in the form of dip-coated liquid films on a silicon substrate, analyzed on a Magna IR Spectrometer 750 from Nicolet Instrument Corp. FTIR was completed in the reflectance mode at a 45° incidence angle from 600 to 4000 cm^{-1}. Spectra of the solvent (Figure S1), PVP in 2-methoxyethanol solution (Figure S2), and control sol without PVP (Figure S3) were collected for reference purposes. They can be found in the Supporting Information. Sampling of the Ta_2O_5 precursor sol (Figure 3, Figure S5) and control sol without acetylacetone (Figure 4, Figure S6) was conducted periodically, starting at the end of sol synthesis and continuing until the 20th day. Samples were Si <111> substrates (acetone−isopropanol rinsed and air-dried) dip-coated in the respective solutions at the indicated points in time using an in-house dipcoater (withdrawal rate = 5 in./min).

Table 1 lists the peaks seen in Figure 3 and their proposed assignments. The spectrum in Figure 3 is very similar to that of 2-methoxyethanol[35] (Figure S1). However, there are extra peaks, a C=O stretch at 1686 cm^{-1}, a 1297 cm^{-1} C−N stretch attributable to PVP molecule, peaks at 1603, 1540, 650, and 770 cm^{-1} attributable to Ta−O or Ta−O−C modes,[26,34] and peaks at 1139, 1083, and 2080−2250 cm^{-1} associated with Si−O and SiH stretches from the silicon substrate.

Note that the C=O peak in our spectrum is at 1686 cm^{-1}. Perjessey and Engberts[32] found that the position of the CO peak is very sensitive to the hydrogen bonding in lactams. The CO peak in gas-phase 2-pyrolidinone is at 1759 cm^{-1} and at 1734 cm^{-1} in dilute hexane solution. As the 2-pyrolidinone concentration increases in hexane solution, a new peak appears below 1700 cm^{-1} associated with hydrogen-bonded dimers. The peak shifts linearly with concentration, so the peak lies at 1689 cm^{-1} in liquid 2-pyrolidinone. A further shift to 1674 cm^{-1} is seen when 2-pyrolidinone is dissolved in CCl_3D due to strong hydrogen bonding to the deuterated chloroform. Perjessey and Engberts interpreted these results as suggesting that there were two types of hydrogen bonding in solutions containing 2-pyrolidinone: hydrogen bonding due to dimer formation and linear hydrogen bonding with a solvent or other species. Generally, the dimers give CO vibrations above 1690 cm^{-1}, whereas hydrogen bonds to solvents give CO vibrations below 1690 cm^{-1}.

The CO vibration in Figure 3 is at 1686 cm^{-1}. This is the middle of the range expected for hydrogen-bonded 2-pyrolidinone. Therefore, we propose that the PVP is hydrogen-bonded. Further, the observed frequency is slightly into the region associated with hydrogen bonding with solvents. Therefore, the implication of the data in Figure 3 is that the PVP is likely hydrogen-bonded to the solvent and other PVP molecules.

The results in Figures 3 and 4 also show that there is very little change in the IR spectrum on the sols during aging. The day = 0 spectrum is virtually identical to the spectrum of 2-methoxyethanol[35] except for 1297 cm^{-1} C−N and 1686 cm^{-1} C=O stretch modes due to PVP. With time, OH and methoxy CH_2 and CH_3 bands broaden out, leaving only the 1472 cm^{-1} CH_2 scissoring, 1686 cm^{-1} C=O, and CH_2 bands at ∼1100 cm^{-1} distinctly visible.[25,27] Two bands at 650 and

(25) Smith, B. *Infrared Spectral Interpretation: A Systematic Approach*; CRC Press: Boca Raton, FL, 1999.
(26) Phule, P. P. *J. Mater. Res.* **1993**, *8* (2), 334−338.
(27) Coates, J. Interpretation of Infrared Spectra, A Practical Approach. In *Encyclopedia of Analytical Chemistry*; Meyers, R. A., Ed.; John Wiley & Sons: Chichester, U.K., 2000; pp 10815−10837.
(28) Kozuka, H.; Higuchi, A. *J. Mater. Res.* **2001**, *16* (11), 3116−3123.
(29) Coleman, W. M., III.; Gordon, B. M. *Appl. Spectrosc.* **1989**, *43* (6), 1008−16.
(30) Coleman, W. M., III; Gordon, B. M. *Appl. Spectrosc.* **1988**, *42* (1), 108−13.
(31) Coleman, W. M.; Gordon, B. M. *Appl. Spectrosc.* **1987**, *41* (5), 886−9.
(32) Perjessy, A.; Engberts, J. B. F. N. *Monatsh. Chem.* **1995**, *126* (8/9), 871−88.
(33) Warshel, A.; Levitt, M.; Lifson, S. *J. Mol. Spectrosc.* **1970**, *33* (1), 84−99.
(34) Kelly, P. V.; Mooney, M. B.; Beechinor, J. T.; O'Sullivan, B. J.; Hurley, P. K.; Crean, G. M.; Zhang, J. Y.; Boyd, I. W.; Paillous, M.; Jimenez, C.; Senateur, J. P. *Adv. Mater. Opt. Electron.* **2000**, *10* (3−5), 115−122.
(35) NIST *NIST Chemistry WebBook*; http://webbook.nist.gov/cgi/cbook.cgi?ID=C109864&Units=SI&Type=IR-SPEC&Index=1#IR-SPEC.

Table 1. Comparison of the FTIR Peaks in Figure 3 to Those of 2-Pyrolidinone (2PY) and 2-Methoxyethanol (2ME)[a]

peak from Figure 3 (cm^{-1})	2ME	2PY gas	hydrogen bonded 2PY	assignment
1026	1014−1034[25−27]			CH_2 undefined[25,27]
1338	1338†			H−O in-plane bend[25−27]
	1349[25−27]			
1375	1375†			H−O in-plane bend[25−27]
	1371[25−27]			
1444	1444†			CH_3 umbrella mode[25,27]
	1449[25−27]			
1473	1473†			CH_2 scissoring[25,27]
	1474[25−27]			
2839	2839†			CH_2 sym stretch[25,27]
	2839[25−27]			
2899	2899†			CH_2 sym stretch[25,27]
	2903[25−27]			
2956	2965†			CH_3 asymmetric stretch[25,27]
	2952[25−27]			
3496−3650	3630[25−27]			O−H stretch[22,25−28]
	3496−3650 †			
1140				Si-O stretch[25,27]
1083				Si-O stretch[8,25,27]
2080−2250				Si-H stretch[25,27]
1686		1759[29−31]	1674−1700[32]	C═O stretch[22,25,27,28]
1297		1288		C−N−H stretch[22,25,27,28]
		1305		
1383		1384[33]		C−H bend[22,27,28]
1099−1053				Ta−O−C[8,26,34]
<1000				Ta−O (stretch, bend and torsion modes)[8,26,34]

[a] The values with a dagger (†) are our measurments. The others are from the literature.

770 cm^{-1} attributable to Ta−O or Ta−O−C modes are present but broad and not as distinct as observed for the sol precursor.[26,34] The sol visibly turns turbid with time. The sol had solidified into a gel after the 12th day. Beyond the 12th day, the gels were still able to yield thick films for analysis by dip-coating Si <111> substrates as performed for the solution phase. Subsequent spectra do not show any deviation.

NMR Analysis. We also used ^1H and ^{13}C NMR to examine the changes in the sol prior to deposition. The analysis was performed using Varian UNITY 400 and Varian UNITY 500 systems. Wilmad 528-PP-7 sample tubes were used. This analysis was important in determining what ligands are attached to the metal center at the end of the synthesis, as well as the fate of the exchanged hydrocarbon groups.[36,37] NMR sampling was conducted daily over a period of 10 days starting at the end of sol synthesis, and thereafter every 2 days until the 20th day from the end of synthesis. The NMR standard used was deuterated chloroform 99.8 at % D with 1% (v/v) TMS. The different samples analyzed were as follows:

- Sol synthesized above (Figure 1)
- Control sol synthesized as above but without PVP
- All the above but with $CaSO_4$(s) pellet acting as H_2O scavenger
- Control sol synthesized as above but without acetylacetone

Figure 5 shows a ^1H NMR spectrum of a fresh sol before deposition. One observes the ^1H spectrum is of a characteristic 2-methoxyethoxide type of coordination.[36,37] The triplet at 3.7 ppm on the ^1H spectrum corresponds to a CH_2 hydrogen of a carbon bound to another CH_2 whose hydrogen signal appears at about 3.48 ppm (triplet) and is bound to an O atom.[36] The singlet at 3.38 ppm corresponds to CH_3 hydrogen bound to an oxygen atom.

The NMR spectra suggest that the ethoxide ligands around the Ta metal center are exchanged for the $OCH_2CH_2OCH_3$ ligand. There is no trace of any ethoxide/ethanol, and hence we can conclude that the exchanged ethoxide ligands are removed as ethanol during the vacuum evaporation stage of synthesis. The suggested product is $Ta(OCH_2CH_2OCH_3)_x$ via the reaction[4,9,38−40]

$$Ta(OCH_2CH_3)_5(l) + xHOCH_2CH_2OCH_3(l) \rightarrow Ta(OCH_2CH_2OCH_3)_x(l) + 5HOCH_2CH_3(l)$$

^1H NMR spectrum of 2-methoxyethanol yields a quartet centered at 3.7 ppm. The occurrence of a triplet for this sample suggests the deprotonation of the 2-methoxyethanol OH groups due to extensive hydrogen bonding. Presence of the Ta−O and Ta−O−C bonds is verified by the FTIR bands at <1000 cm^{-1}, see Figure 3 and Table 1.

Figure 6 shows the ^{13}C NMR spectrum of the sol. The ^{13}C spectrum confirms the above coordination with the methyl carbon at 58.8 ppm, the oxygen bonded CH_2 carbon at 73.6 ppm, and the adjacent CH_2 carbon at 61.7 ppm (Figure 6).[36] NMR spectra of samples with $CaSO_4$ pellet yielded identical spectra to the peaks expected for a 2-methoxyethanol group. Again, this shows that the ethoxy in the precursor has been replaced by 2-methoxyethyl groups in the sol.

(36) Kim, Y.; Chae, H. K.; Lee, K. S.; Lee, W. I. *J. Mater. Chem.* **1998**, *8* (11), 2317−2319.
(37) Werndrup, P.; Verdenelli, M.; Chassagneux, F.; Parola, S.; Kessler, V. G. *J. Mater. Chem.* **2004**, *14* (3), 344−350.
(38) Clem, P. G.; Jeon, N. L.; Nuzzo, R. G.; Payne, D. A. *J. Am. Ceram. Soc.* **1997**, *80* (11), 2821−2827.
(39) Brinker, C. J.; Scherer, G. W. *Sol−Gel Science−The Physics and Chemistry of Sol−Gel Processing*. Academic Press: San Diego, CA, 1990.
(40) Hubert-Pfalzgraf, L. G. *New J. Chem.* **1995**, *19*, 727−750.

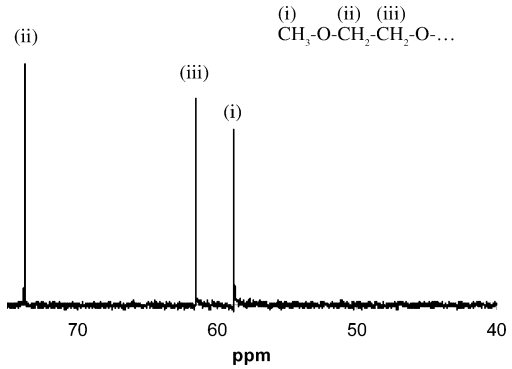

Figure 6. ^{13}C NMR of a fresh sol formed from $Ta(OC_2H_5)_5$, isopropanol, PVP, acetylacetone, and 2-methoxyethanol.

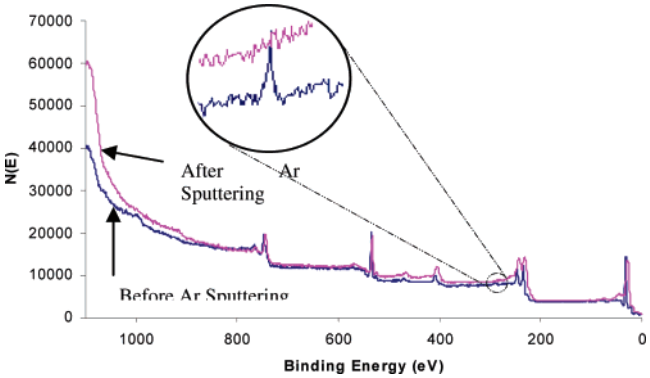

Figure 7. XPS scan of a Ta_2O_5 film calcined in O_2 at 900 °C: 743 eV, O $KL_{23}L_{23}$; 531 eV, O 1s; 401 eV, Ta $4p_{3/2}$; 285 eV, C1s; 240 eV,Ta $4d_{3/2}$; 229 eV, Ta $4d_{5/2}$; 24 eV, Ta$4f_{5/2}$.

Table 2. XPS Table of Assignment.

	binding energy (eV)	surface atomic concn (%)	interior atomic concn (%)
O 1s	531	63.7	70.1
C 1s	285	13.8	0.9
Ta $4f_{5/2}$	24	22.6	29

Another interesting observation is that we do not observe any peaks associated with PVP in the NMR. Campbell[41] discusses this effect in some detail. Large molecules show weak NMR signals, because they tumble only slowly, see Foster et al.[42] With hydrogen bonding, the peaks disappear.

There was no variation in the ^1H and ^{13}C spectra obtained from the aging samples (Figures 5 and 6). Spectra obtained from the control samples were similar to the spectra of the actual precursor.

XPS Analysis. X-ray photoelectron spectroscopy was used to investigate the residual carbon content of the Ta_2O_5 films after calcination. Analysis was done on a PHI 5400 XPS system (Mg Kα X-ray source). The oxide upper surface and interior of the film (surface was sputtered with Argon for 15 min) were both analyzed (Figure 7). XPS was also used to reveal the Ta:O:C atomic ratio (Table 2).

X-ray Diffraction Analysis. Identification of the phases of the resulting oxide film was performed via XRD on a Rigaku DMAX XRD system with Cu (Kα) radiation (Figure 8).

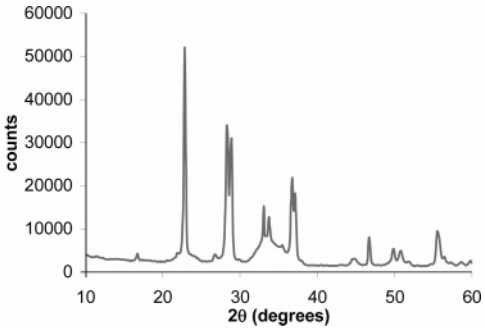

Figure 8. XRD spectrum of Ta_2O_5 film on Si <100> calcined in O_2 at 900 °C.

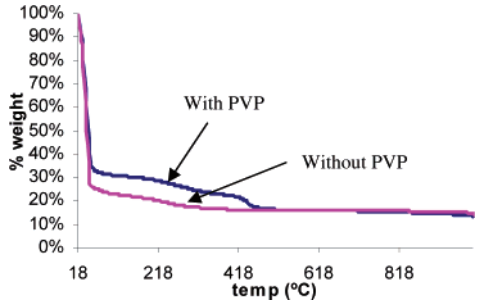

Figure 9. TGA analysis of Ta_2O_5 sol precursor with PVP and without PVP.

Table 3. Table of Miller Indices

2θ (deg)	(*h k l*)
22.819	(0 1 0)
28.244	(12 0 1)
28.733	(0 0 2)
32−35	Si (100) substrate
37.003	(0 1 2)
46.611	(0 2 0)
49.693	(24 0 0)
50.604	(12 0 3)
55.397	(12 2 1)

TGA Analysis. Thermogravimetric analysis was performed to elucidate the change in physical properties that occurs through the calcination cycle to yield the final oxide film. Analysis was performed on a TGA7/DSC7 Perkin-Elmer system. Samples were heated from ambient temperature to 900 °C at a rate of 1.6 °C/min under a steady O_2 flow of 20 cm^3/min and finally held at 900 °C for 10 h (Figure 9).

Discussion

The results in this paper explain the qualitative features of the results in our previous paper. To review, in our previous paper,[23] we found that thick, crack-free films could be formed by spin coating a sol containing PVP or PVP and acetylacetone, whereas many cracks formed upon calcination in the absence of PVP and acetylacetone. With PVP alone, the films were not stable to thermal cycling, but when we added acetylacetone too, the films could be thermally cycled. We also found that the best films were formed from fresh sols. Aged sols tended to give grainy structures that were not suitable for the application. In contrast, when fresh sols were used, the resultant films would meet the needs of our application.

The results in Figures 2 and 3 explain why this is so. As discussed earlier, the IR spectra in Figure 3 suggests that

(41) Campbell, D. W. J. R. *Polymer Characterization: Physical Techniques*; Chapman and Hall: New York, 1989; p 362.
(42) Foster, P.; McElroy, A.; Amero, C. D. *Biochemistry* **2007**, *46* (2), 331−340.

PVP forms hydrogen bonds with the solvent and other PVP molecules. The CO peak in the films is in a position that Perjessey and Engberts[32] report as being characteristic of pyrolidinone hydrogen-bonded to solvent molecules. Thus, the IR provides strong evidence for hydrogen bonding in the sol.

The spectroscopy does not tell us exactly what the PVP does to the sol. However, the presence of strong hydrogen bonding combined with an absence of discernible PVP peaks in NMR suggests that the PVP is in a hydrogen-bonded network. We suppose that this network slows the release of solvent and holds the sol together until calcination begins.

Acetylacetone seems to have a different effect. The data in Figure 2a shows that the addition of acetylacetone causes a phase transition in the film. The data in Figure 2a shows that round tantalum containing nodules form when acetylacetone is added to the sol. This compares to a continuous film in the absence of acetylacetone (Figure 2b). Experimentally, the films formed with acetylacetone are more stable to temperature cycling than the films formed in the absence of acetylacetone, even though the IR, NMR, XPS, and XRD data in Figures 3-8 do not reveal any significant differences in the chemistry of the films. Therefore, the changes in behavior that are observed must be associated with changes in the microstructure of the film. We suppose that films with a fine grain structure are formed when the film in Figure 2a is calcined. The fine grain structure would facilitate stress relief during temperature cycling.

Another key point is that the nodules grow as the sol ages. See Figure 2. Analysis of sols at different points in time via both NMR and FTIR does not show any change in chemical composition as the sol ages (Figures 3−6). This suggests that the difference observed in film thickness and microstructure from sols of different age is a physical effect, namely the growth of the tantalum containing nodules. The polycondensed oxide particles are about 822 nm in diameter (Figure 2a). As time goes by, there is further polycondensation of the oxide network, giving larger particle sizes in the films derived from sols subjected to greater aging (1.11 μm; Figure 2b). SEM micrographs of green films from aged sols show particle sizes of about 2−5 μm diameter (Figure 2c). The calcined Ta_2O_5 films also echo this variation in microstructure.[23] Evidently, the growth of the nodules leads to larger grains in the resulting film, which leads to poorer film properties.

The results here also reveal some interesting features of the chemistry of sol formation. The sol precursor exhibits FTIR bands at 1603 and 1540 cm^{-1} that are absent from the control and other comparison spectra. These bands fall within the region in which Ta-coordinated acetylacetanate modes occur and also have the expected 63 cm^{-1} separation.[26] This suggests that there are mixed ligands around the Ta center, though the acetylacetanate ligands are undetectable by NMR experiments, implying that they are significantly H-bonded to the PVP or to the growing M−O−M network. Therefore, we can conclude that the actual ligand-exchange reaction that occurs during the sol synthesis is as follows

$$Ta(OCH_2CH_3)_5(l) + xHOCH_2CH_2OCH_3(l) \rightarrow Ta(OCH_2CH_2OCH_3)_x(l) + 5HOCH_2CH_3(l)$$

$$Ta(OCH_2CH_2OCH_3)_x(l) + yC_5H_8O_2(l) \rightarrow Ta(OCH_2CH_2OCH_3)_{x-y}(C_5H_8O_2)_y(l) + 2yHOCH_2CH_3(l)$$

General polycondensation sequence of reaction is as follows[4,39,40]

$$\text{Hydrolysis: } 2M(OR)_4 + 2H_2O \rightarrow 2(RO)_3M{-}OH + 2ROH$$

Subsequent condensation reactions involving the hydroxyl groups yield networks composed of inorganic oxide (M−O−M) linkages.

$$\text{Olation: } 2(RO)_3M{-}OH \rightarrow (RO)_3M{-}O{-}M(OR)_3 + H_2O$$

$$\text{Oxolation: } (RO)_3M{-}OH + M(OR)_4 \rightarrow (RO)_3M{-}O{-}M(RO)_3 + ROH$$

The extensive H-bonded network made up of PVP, solvent, and hydrolysis product allows for thicker films than those derived from binder-free sols because of the increased mechanical tolerance. The mixed ligands present result in a directionally different rate of hydrolysis around the metal center, with the acetylacetanate groups being more slowly removed because of their charge-stabilizing effect. The resulting difference in growth rates is likely to force the M−O−M network formation to take on the globular microstructure. This type of microstructure is absent in films deposited from the acetylacetone free sol (Figure 2d−f). With time, the acetylacetanate ligands undergo polycondensation as well, albeit at a much slower rate, hence the denser, thinner films with larger spheroidal particles. Acetylacetone has been observed in other studies to not only slow down the rate of hydrolysis and polycondensation but also to significantly influence the morphology and crystallinity of the final product of the sol gel synthesis.[43,44]

TGA results show an initial drop in mass up to 50 °C attributed to solvent evaporation (Figure 9). Between 60 and 500 °C, there is a change in the rate of decrease in percent weight, with the PVP-assisted sample showing a slower rate of change than the sample without PVP. There is a significant increase in the rate of decrease of percent weight at 450 °C, which is attributable to a change in structure from amorphous to orthorhombic Ta_2O_5. Beyond 500 °C, the rate of change in percent weight is similar for both samples. This supports the hypothesis that the presence of PVP serves to relieve stresses within the film upon thermal treatment up to about 500 °C when all the binder is pyrolized.[22,28] The slower rate of decrease in percent weight signifies slower change in the film microstructure, a plasticity that allows differential expansion between the film particles and substrate with minimal or no cracking of the film.

XPS data reveals 13.8% carbon content that is reduced to 0.9% upon sputtering with argon, confirming ambient contamination as the carbon source. This shows that the

(43) Nakagawa, K.; Wang, F. M.; Murata, Y.; Adachi, M. *Chem. Lett.* **2005**, *34* (5), 736−737.
(44) Maslosh, V. Z.; Kotova, V. V.; Maslosh, O. V. *Russ. J. Appl. Chem.* **2002**, *75* (8), 1369−1370.

removal of PVP is complete and there is no residual carbon. The Ta:O ratio confirms atomic coordination as Ta_2O_5 (Figure 7 and Table 1).

XRD pattern identifies the calcined film obtained as orthorhombic Ta_2O_5. The spectrum matches ICSD card 97-004-7493 (Figure 8 and Table 2).

Conclusion

PVP has been shown to be an effective binder material in the sol−gel synthesis of thick, crack-free Ta_2O_5 films for high-temperature applications. This study was undertaken to investigate the interaction of PVP, 2-methoxyethanol, acetylacetone, and metal center in the sol precursor via NMR, FTIR, TGA, XPS, SEM, and XRD analytical tools. We found that the PVP forms a hydrogen-bonded network, whereas acetylacetone promotes microparticle formation. This type of microstructure effectively relieves stresses that occur in the film during solvent removal and calcination processes. The resulting films are found to be stable and crack-free with a maximum thickness of 2.4 μm for films deposited from freshly prepared sols. With time, there is continued polycondensation of the Ta−O−Ta network, yielding denser, thinner films with particles of larger diameter.

Acknowledgment. This work was supported by the Department of Defense Multidisciplinary University Research Initiative (MURI) program administered by the Army Research Office under contract DAAD19-01-1-0582. Any opinions, findings, and conclusions or recommendations expressed in this publication are those of the authors and do not necessarily reflect the views of the Department of Defense or the Army Research Office. SEM, XRD and XPS analysis was carried out in the Center for Microanalysis of Materials, University of Illinois, which is partially supported by the U.S. Department of Energy under grant DEFG02-91-ER45439.

Supporting Information Available: FTIR and XPS spectra. This material is available free of charge via the Internet at http://pubs.acs.org.

CM062231W